observed TRPV3 protein expression in a majority of keratinocytes and detected abundant TRPV3-like responses in the presence of 2-aminoethoxydiphenyl borate (2-APB), a compound that activates and sensitizes TRPV3 (*8*, *18*, *19*). Consistent with these reports, we observed that pretreatment with 100 μM 2-APB strongly potentiated heat and camphor responses in keratinocytes (Fig. 4, C and D), whereas camphor was not capable of sensitizing 2-APB responses (n = 3) (*9*). Together, these studies imply that TRPV3 is present in a majority of cultured keratinocytes.

We next compared the camphor- and heat-induced currents of wild-type and TRPV3$^{-/-}$ littermate keratinocytes. The majority of wild-type keratinocytes showed gradually increasing current responses with repeated 37°C pulses at –60 mV, whereas TRPV3$^{-/-}$ keratinocytes showed no responses or some responses with TRPV4-like desensitization (Fig. 4E) (fig. S6B). Responses to repeated application of 5 mM camphor were observed in wild-type but not TRPV3$^{-/-}$ keratinocytes (Fig. 4F). This suggests that TRPV3 is a heat receptor in keratinocytes, that it is the only receptor for camphor in these cells, and that camphor sensitivity is a specific functional marker for TRPV3. Unlike what was observed for keratinocytes, 5 mM camphor failed to evoke sensitizing current responses from capsaicin-sensitive or capsaicin-insensitive DRG neurons from either wild-type mice (n = 43) or TRPV3$^{-/-}$ mice (n = 14) (Fig. 4G).

The residual sensitivity to warm temperatures in TRPV3$^{-/-}$ mice may be due to partial compensation by TRPV4, the only other ion channel known to respond to innocuous heat in culture (*20*, *21*). Consistent with expression analysis, camphor activity was observed in keratinocytes but not in DRG neurons, even with high concentrations of camphor. Therefore, the acute thermosensory phenotype observed in TRPV3$^{-/-}$ mice suggests an important role of skin in temperature sensation. Keratinocytes are not known to "sense" temperature; instead, DRGs are thought to directly sense heat through free nerve endings (*1*). This conclusion is mainly based on the ability of dissected neurons to respond to temperature shifts and on the anatomical observation that no synapses are apparent between free nerve endings and keratinocytes (*22*, *23*). However, a recent study has observed a population of chemosensory cells that form synaptic contacts with trigeminal afferent nerve fibers within the nasal epithelium (*24*). Furthermore, nonsynaptic communication between keratinocytes and nerve fibers can be considered.

References and Notes

1. H. Hensel, *Monogr. Physiol. Soc.* **38**, 1 (1981).
2. A. Patapoutian, A. P. Peier, G. M. Story, V. Viswanath, *Nature Rev. Neurosci.* **4**, 529 (2003).
3. A. M. Peier *et al.*, *Science* **296**, 2046 (2002).
4. G. D. Smith *et al.*, *Nature* **418**, 186 (2002).
5. H. Xu *et al.*, *Nature* **418**, 181 (2002).
6. W. Liedtke *et al.*, *Cell* **103**, 525 (2000).
7. M. Suzuki *et al.*, *Neurosci. Lett.* **353**, 189 (2003).
8. M. K. Chung, H. Lee, A. Mizuno, M. Suzuki, M. J. Caterina, *J. Biol. Chem.* **279**, 21569 (2004).
9. A. Moqrich *et al.*, data not shown.
10. T. Miyakawa, M. Yamada, A. Duttaroy, J. Wess, *J. Neurosci.* **21**, 5239 (2001).
11. J. Reichelt, H. Büssow, C. Grund, T. M. Magin, *Mol. Biol. Cell* **12**, 1557 (2001).
12. H. Todaka, J. Taniguchi, J.-i. Satoh, A. Mizuno, M. Suzuki, *J. Biol. Chem.* **279**, 35133 (2004).
13. J. B. Davis *et al.*, *Nature* **405**, 183 (2000).
14. M. J. Caterina *et al.*, *Science* **288**, 306 (2000).
15. S. E. Jordt *et al.*, *Nature* **427**, 260 (2004).
16. M. Bandell *et al.*, *Neuron* **41**, 849 (2004).
17. B. G. Green, *J. Invest. Dermatol.* **94**, 662 (1990).
18. H. Z. Hu *et al.*, *J. Biol. Chem.* **279**, 35741 (2004).
19. M. K. Chung, H. Lee, A. Mizuno, M. Suzuki, M. J. Caterina, *J. Neurosci.* **24**, 5177 (2004).
20. A. D. Guler *et al.*, *J. Neurosci.* **22**, 6408 (2002).
21. H. Watanabe *et al.*, *J. Biol. Chem.* **277**, 13569 (2002).
22. N. Cauna, *J. Anat.* **115**, 277 (1973).
23. M. Hilliges, L. Wang, O. Johansson, *J. Invest. Dermatol.* **104**, 134 (1995).
24. T. E. Finger *et al.*, *Proc. Natl. Acad. Sci. U.S.A.* **100**, 8981 (2003).

25. We thank M. Bandell, B. Conti, H. Esendencia, P. Garrity, S. Kupriyanov, M. Mayford, A. Peier, L. Reijmers, M. Wood, and J. Watson for input and assistance; M. Caterina for sharing a detailed protocol on primary culture of keratinocytes; T. Bartfai for sharing the thermal gradient platform; and N. Hong, T. Jegla, U. Mueller, and L. Stowers for critical reading of the manuscript. Supported by National Institute of Neurological Disorders and Stroke grants R01NS046303 and R01NS42822. G.M.S. is a recipient of a National Research Service Award postdoctoral fellowship from NIH. A.P. is a Damon Runyon Scholar.

Supporting Online Material

www.sciencemag.org/cgi/content/full/307/5714/1468/DC1
Materials and Methods
Figs. S1 to S6
References

13 December 2004; accepted 4 January 2005
10.1126/science.1108609

OSBP Is a Cholesterol-Regulated Scaffolding Protein in Control of ERK1/2 Activation

Ping-yuan Wang, Jian Weng, Richard G. W. Anderson*

Oxysterol-binding protein (OSBP) is the founding member of a family of sterol-binding proteins implicated in vesicle transport, lipid metabolism, and signal transduction. Here, OSBP was found to function as a cholesterol-binding scaffolding protein coordinating the activity of two phosphatases to control the extracellular signal–regulated kinase (ERK) signaling pathway. Cytosolic OSBP formed a ~440-kilodalton oligomer with a member of the PTPPBS family of tyrosine phosphatases, the serine/threonine phosphatase PP2A, and cholesterol. This oligomer had dual specific phosphatase activity for phosphorylated ERK (pERK). When cell cholesterol was lowered, the oligomer disassembled and the level of pERK rose. The oligomer also disassembled when exposed to oxysterols. Increasing the amount of OSBP oligomer rendered cells resistant to the effects of cholesterol depletion and decreased the basal level of pERK. Thus, cholesterol functions through its interaction with OSBP outside of membranes to regulate the assembly of an oligomeric phosphatase that controls a key signaling pathway in the cell.

Depletion of membrane cholesterol markedly increases the level of pERK in the caveolae and cytosol fractions of cells (*1*). The level of pERK is increased further by simultaneously exposing the cells to epidermal growth factor (EGF), which suggests that cholesterol depletion inactivates a pERK phosphatase. Recently, we identified a cholesterol-regulated phosphatase that has dual specific activity for pERK (*2*). When cellular cholesterol levels are normal, this phosphatase works in tandem with the ERK kinase MEK-1 to regulate the level of pERK in the cell. The phosphatase is a heterooligomer of ~440 kD that derives its dual specific activity from two phosphatases. One is a member of the PTPPBS family of tyrosine phosphatases (*3*), and the other is the serine/threonine phosphatase PP2A (*2*). These two enzymes each depend on the activity of the other to coordinately remove phosphate from both the threonine and the tyrosine residues of pERK. Depletion of cell cholesterol results in the dissociation of PP2A from the PTPPBS member and a loss of dual specific pERK phosphatase activity. Thus, cholesterol appears to act directly or indirectly to control the formation of an oligomer of two phosphatases that together have functionality that neither has alone. Here, we present

Department of Cell Biology, University of Texas Southwestern Medical Center, Dallas, TX 75390–9039, USA.

*To whom correspondence should be addressed. E-mail: richard.anderson@utsouthwestern.edu

evidence that this oligomer is held together through interactions between cholesterol and the OSBP.

The cholesterol dependency of the oligomeric phosphatase complex was demonstrated using HeLa cells expressing a cDNA for the PTPPBS family member HePTP tagged with polyhistidine, myc, and an influenza hemagglutinin peptide (HA). Cells were transfected for 48 hours, incubated in the presence of methyl-β-cyclodextrin (CD) or CD plus cholesterol for 60 min (to remove or retain cholesterol, respectively), and the cytosol was used to purify the HePTP by nickel-nitrilotriacetic acid (Ni-NTA) agarose chromatography. The HA-HePTP-myc-his was eluted with increasing concentrations of imidazole. Peak elution occurred at an imidazole concentration of 80 to 160 mM (Fig. 1A). The HePTP isolated from cells exposed to CD plus cholesterol coeluted with the PP2A phosphatase, whereas PP2A was markedly reduced in fractions of HA-HePTP-myc-his isolated from cholesterol-depleted cells (Fig. 1A).

In transfected cells, lipid, probably cholesterol, was found in the HePTP/PP2A complex (Fig. 1B). HeLa cells expressing HA-HePTP-myc-his were labeled with [^{3}H]-cholesterol and [^{3}H]-palmitic acid. HA-HePTP-myc-his was isolated with Ni-NTA agarose beads and processed for thin-layer chromatography (TLC). Autoradiography showed a single band in the cytosol fraction that comigrated with cholesterol and was absent in CD-treated cells. A slower migrating radioactive band eluted from the Ni-NTA beads with imidazole. This band was also absent from CD-treated cells, which suggests that it was cholesterol. Fourteen different oxysterols that we tested failed to migrate to the same position (table S1). Furthermore, imidazole caused cholesterol to migrate anomalously on TLC (Fig. 1C), and cytosolic [^{3}H]-cholesterol migrated the same when exposed to imidazole (fig. S1). We did not detect any phospholipid or ceramide in the complex.

The presence of cholesterol suggested that the oligomeric phosphatase contained a sterol-binding protein. Initially, we thought the bound lipid that migrated slower on TLC plates (Fig. 1B) was an oxysterol, which prompted us to see whether the oligomer contained OSBP. We purified the oligomer from HeLa cells expressing HA-HePTP-myc-his and processed the sample for immunoblotting (Fig. 2A). The complex clearly contained endogenous OSBP and PP2A. Depleting cells of cholesterol caused the loss of both proteins from the complex. HA-HePTP-myc-his lacking a 15 amino acid segment called the kinase interaction motif (KIM) domain (ΔKIM-HePTP) (*4*) did not interact with endogenous OSBP (Fig. 2B).

Thus, OSBP may represent a cholesterol-binding component of the endogenous complex that we originally purified from HeLa cells (*2*). We used monoclonal antibody (mAb) OSBP to immunoblot the fractions from the columns used for purification (Fig. 2, C and D). Even though this antibody was not sensitive enough to detect OSBP in cytosol fractions, a strong signal was seen in fractions from both the Mono Q (Fig. 2C) and the gel filtration columns used to purify the oligomer (Fig. 2D). We could also co-immunoprecipitate endogenous OSBP from the gel-filtration fractions with α-PP2A immunoglobulin G (IgG). In addition, bacterially expressed OSBP bound [^{3}H]-cholesterol (Fig. 2E and fig. S2). Remarkably, the bound [^{3}H]-cholesterol was displaced by cholesterol but not by 25-hydroxycholesterol (Fig. 2E), which suggests that oxysterols and cholesterol bind to different sites on OSBP.

If OSBP interacts with HePTP, coexpressing the two should cause more oligomer to form because cells have excess PP2A (Fig. 3A). Cells were transiently transfected with either HA-HePTP-myc-his, OSBP, or the combination, and HA-HePTP-myc-his was purified. In cells expressing HA-HePTP-myc-his alone, the bound HA-HePTP-myc-his was enriched in endogenous OSBP relative to the unbound cytosol. Some $PP2A_B$ also coeluted, indicating the presence of oligomer. Little OSBP bound to Ni-NTA from cytosol of cells expressing OSBP alone. By contrast, cells coexpressing HA-HePTP-myc-his and OSBP had dramatically more bound OSBP and $PP2A_B$. The same result was obtained if the polyhistamine tag was put on OSBP instead of HePTP (fig. S3). OSBP lacking the pleckstrin homology (PH) domain (ΔPH-OSBP) was unable to oligomerize with HePTP and PP2A, whereas mutating the highly conserved valine 522, serine 523 signature region (VS-OSBP) to alanine had no effect (fig. S3).

We postulate that cholesterol bound to OSBP is what holds the oligomer together. If so, then the quantity of oligomer (cholesterol, HePTP, OSBP, and PP2A) present in cells should be a function of the amount of OSBP. We expressed the same amount of HA-HePTP-myc-his in two sets of cells expressing 10-fold different amounts of OSBP (Fig. 3B). The cells were labeled with [^{3}H]-cholesterol overnight before processing for purification of HA-HePTP-myc-his. Immunoblots showed that nearly equal amounts of HA-HePTP-myc-his were present. Markedly more OSBP and PP2A were present in fractions from cells expressing the higher amount of OSBP. Moreover, the fraction with the highest amount of OSBP contained 5 times as much radioactive lipid as the corresponding fraction from cells expressing low levels of OSBP. We conclude that OSBP

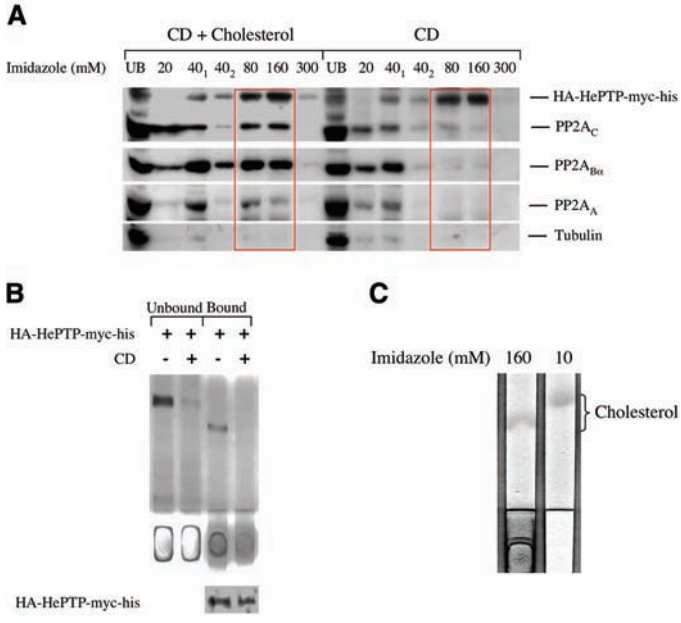

Fig. 1. Isolation of the cholesterol-regulated HePTP/PP2A oligomer using Ni-NTA chromatography. (**A**) HeLa cells expressing HA-HePTP-myc-his were incubated in the presence of 1% CD or a mixture of 1% CD and 200 μg/ml cholesterol for 1 hour at 37°C. The cells were washed and the cytosol isolated. Six milligrams of cytosol was mixed with Ni-NTA beads and incubated for 3 hours at 4°C. The beads were pelleted, loaded on a column, and washed with the indicated concentrations of imidazole. Sixty micrograms of the unbound (UB) protein and equal volumes of each eluate were processed for immunoblotting with antibodies that recognize the indicated proteins. (**B**) HeLa cells expressing HA-HePTP-myc-his were labeled with [^{3}H]-cholesterol and [^{3}H]-palmitic acid. Cytosol was prepared from cells that had been incubated in the presence or absence of 1% CD for 1 hour at 37°C. Equal amounts of cytosol (3 mg) were processed for isolation of the oligomer on Ni-NTA beads. Fifty microliters of the unbound fraction and 500 μl of the bound fraction were processed for lipid extraction. The lipids were separated by TLC and the radioactivity detected by autoradiography. A 50-μl sample of the bound fraction was also processed for immunoblotting to detect HA-HePTP-myc-his. (**C**) Fifty micrograms of unlabeled cholesterol was mixed with buffer B containing either 10 mM or 160 mM imidazole, extracted, and loaded onto a TLC plate, and the lipids were separated using the same condition as in (B). Cholesterol was visualized by iodine staining.

drives assembly of the two phosphatases plus cholesterol into an oligomeric complex.

OSBP is known as an oxysterol-binding protein (*5*), which raises the possibility that oxysterols affect oligomer assembly. Cytosol from HeLa cells expressing OSBP and HA-HePTP-myc-his was mixed with either 25-hydroxycholesterol or cholesterol before purifying the HA-HePTP-myc-his (Fig. 3C). The HA-HePTP-myc-his isolated from the cholesterol-treated cytosol contained both OSBP and PP2A, indicating the presence of the oligomeric phosphatase. By contrast, neither protein was associated with HA-HePTP-myc-his isolated from 25-hydroxycholesterol–treated cytosol. Previous studies have shown that incubating cells in the presence of 25-hydroxycholesterol increases pERK but not phosphorylated c-Jun N-terminal kinase (pJNK) (*6*, *7*). We found that exposing cytosol to 25-hydroxycholesterol inhibited pERK dephosphorylation activity (fig. S4).

Immunoprecipitates of either HePTP or PP2A have dual specific phosphatase activity for pERK (*2*). HeLa cells expressing OSBP-myc-his and HA-HePTP were processed to measure pERK phosphatase activity in OSBP immunoprecipitates (Fig. 4A). Dual specific phosphatase activity was measured by using immunoblotting to detect either the pY or the pT in a pERK2-GST (glutathione S-transferase) substrate. Incubation of pERK2-GST in the presence of immunoprecipitated OSBP caused a marked reduction in the level of both pY and pT. The presence of either vanadate or okadaic acid inhibited dephosphorylation of both residues. No phosphatase activity was detected when α-myc IgG was replaced with a nonimmune IgG. Thus, antibodies against tagged HePTP, OSBP, and untagged PP2A all immunoprecipitate the oligomeric phosphatase activity (*2*).

Further evidence that the three proteins in the complex interact functionally came from the chance observation that the pT-specific pERK mAb recognized OSBP in the immunoprecipitated oligomer (Fig. 4A). Vanadate reduced pT-specific mAb pERK binding, which suggests that it stimulated PP2A to dephosphorylate a phosphothreonine residue in OSBP. Indeed, vanadate-dependent loss of pT-specific mAb pERK immunoblotting of OSBP was blocked by okadaic acid (fig. S5B). We obtained the same results when mAb pThr was substituted for pT-specific mAb pERK (Fig. 4A). We observed the same phenomenon with purified endogenous oligomeric phosphatase. Thus, an interaction occurs in the oligomer between HePTP and PP2A that controls OSBP phosphorylation.

We also found that incubating cytosol in the presence of CD caused a loss of PP2A from the oligomer (fig. S5A), which indicates that removal of cholesterol from the cytosol causes a partial disassembly of the phosphatase. As expected, vanadate no longer stimulated dephosphorylation of pOSBP in immunoprecipitated complexes lacking PP2A (fig. S5B). These results suggest that cytosolic cholesterol is required for stability of the oligomer.

We could not be certain whether HePTP is the PTPPBS family member in the endogenous HeLa cell oligomeric phosphatase because of the lack of an appropriate antibody. Nevertheless, when we adjusted the amount of pERK phosphatase activity by increasing or decreasing the amount of OSBP, the level of endogenous pERK changed (Fig. 4, B and C). The level of pERK in both fractions was markedly lower in cells expressing wild-type and VS-OSBP compared with cells expressing ΔPH-OSBP (Fig. 4B). Because only OSBP and VS-OSBP interact with HePTP (fig. S3), increasing the amount of oligomeric phosphatase reduces endogenous pERK levels. Endogenous pERK phosphatase was reduced by RNA interference (RNAi) of OSBP mRNA (Fig. 4C). Cells were exposed to two small interfering RNAs (siRNAs) directed against different regions of the OSBP mRNA and one control siRNA directed against an irrelevant mRNA before processing for immunoblotting and reverse transcription polymerase chain reaction (RT-PCR). Reducing the mRNA for OSBP resulted in a marked increase in the amount of pERK in the cell.

Increasing the amount of oligomeric phosphatase blocked the effects of cholesterol depletion on pERK dephosphorylation. HeLa cells expressing HA-HePTP and OSBP, but not HA-HePTP alone, have elevated amounts of oligomeric phosphatase (Fig. 3A). Incubating either set of cells in the presence of the MEK-1 inhibitor PD98059 for 10 min to

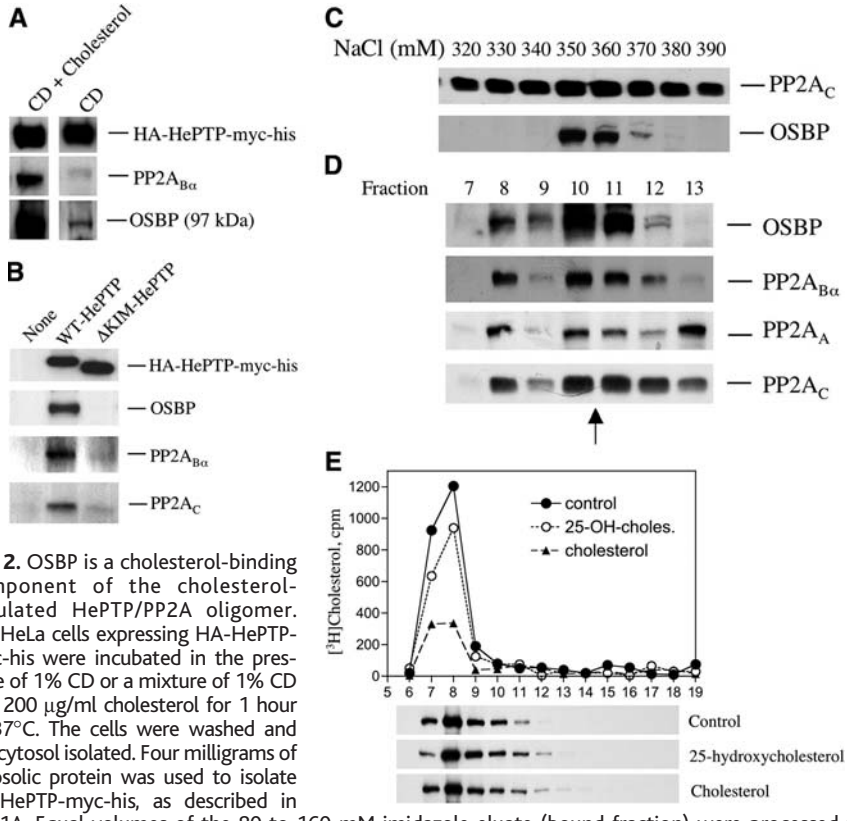

Fig. 2. OSBP is a cholesterol-binding component of the cholesterol-regulated HePTP/PP2A oligomer. (**A**) HeLa cells expressing HA-HePTP-myc-his were incubated in the presence of 1% CD or a mixture of 1% CD and 200 μg/ml cholesterol for 1 hour at 37°C. The cells were washed and the cytosol isolated. Four milligrams of cytosolic protein was used to isolate HA-HePTP-myc-his, as described in Fig. 1A. Equal volumes of the 80 to 160 mM imidazole eluate (bound fraction) were processed for immunoblotting. (**B**) HeLa cells expressing either nothing, HA-HePTP-myc-his, or HA-HePTP-myc-his lacking the KIM domain were processed to isolate his-tagged proteins as described using a 2-mg sample of cytosol. The protein from an equal volume of the bound fraction was processed for immunoblotting with the indicated antibodies. (**C**) HeLa cell cytosol (10 mg) was loaded on a Mono Q column and washed extensively with 250 mM NaCl as described (*2*). Fractions from the column were eluted with a linear 250 to 450 mM NaCl gradient. Equal volumes of the indicated fractions were processed for immunoblotting. (**D**) The 350 to 380 mM fractions were pooled and processed for purification by gel filtration as described (*2*). Fractions (1 ml) were collected and processed for immunoblotting. The peak fraction for ferritin (440 kD) is marked with an arrow. (**E**) A Ni-NTA–purified, bacterially expressed OSBP/[^{3}H]-cholesterol complex (500 μl) was mixed with either 4 μl of ethanol (filled circles) or 4 μl of ethanol containing 1 mg/ml of either cholesterol (triangles) or 25-hydroxycholesterol (open circles) (20 μM final concentration) and incubated overnight at 4°C. The samples were then separated by gel filtration and each fraction assayed either for radioactivity or OSBP using mAb α-V5.

block phosphorylation of ERK caused a marked reduction in the level of endogenous pERK (Fig. 4D). When cells expressing only HA-HePTP-his were depleted of cholesterol, the loss of pERK was markedly inhibited. By contrast, cholesterol depletion had little effect on endogenous pERK dephosphorylation in cells expressing both OSBP and HA-HePTP.

Although we cannot rule out the possibility that other proteins in the oligomeric complex mediate cholesterol regulation, assembly of the oligomeric pERK phosphatase

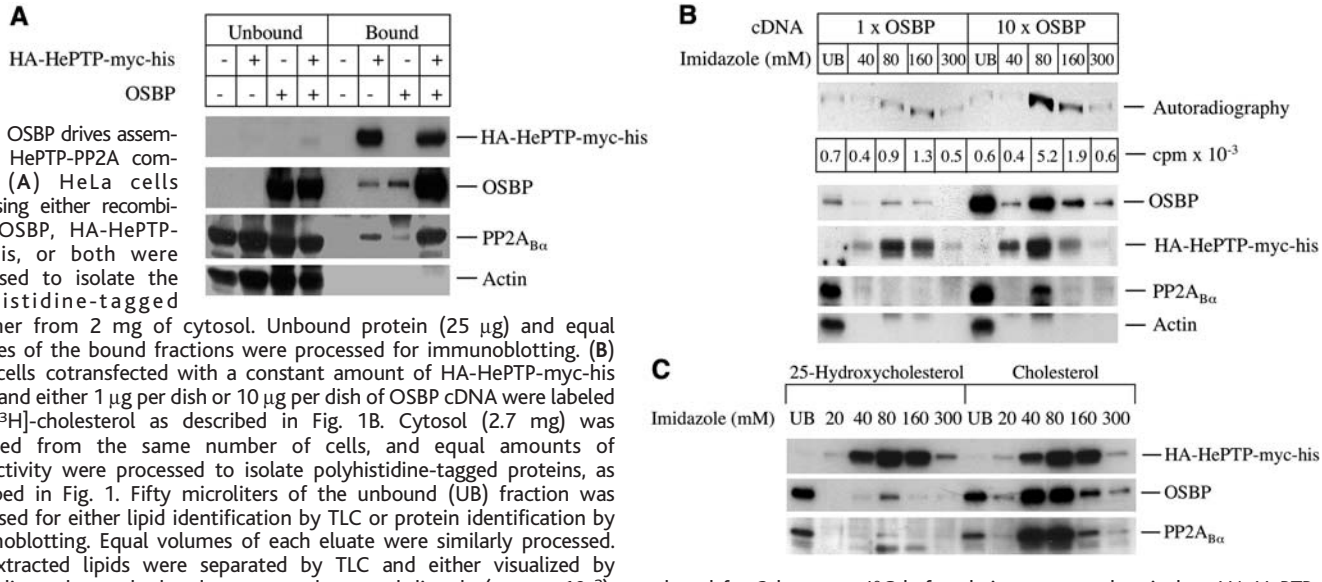

Fig. 3. OSBP drives assembly of HePTP-PP2A complex. (**A**) HeLa cells expressing either recombinant OSBP, HA-HePTP-myc-his, or both were processed to isolate the polyhistidine-tagged oligomer from 2 mg of cytosol. Unbound protein (25 μg) and equal volumes of the bound fractions were processed for immunoblotting. (**B**) HeLa cells cotransfected with a constant amount of HA-HePTP-myc-his cDNA and either 1 μg per dish or 10 μg per dish of OSBP cDNA were labeled with [^{3}H]-cholesterol as described in Fig. 1B. Cytosol (2.7 mg) was prepared from the same number of cells, and equal amounts of radioactivity were processed to isolate polyhistidine-tagged proteins, as described in Fig. 1. Fifty microliters of the unbound (UB) fraction was processed for either lipid identification by TLC or protein identification by immunoblotting. Equal volumes of each eluate were similarly processed. The extracted lipids were separated by TLC and either visualized by autoradiography or the band cut out and counted directly (cpm × 10^{-3}). (**C**) Cytosol (2 mg) from HeLa cells expressing HA-HePTP-myc-his and OSBP was mixed with Ni-NTA beads and incubated in the presence of either 20 μM 25-hydroxycholesterol or 20 μM cholesterol dissolved in ethanol for 3 hours at 4°C before being processed to isolate HA-HePTP-myc-his, as described in Fig. 1. A 25-μg sample of UB proteins and equal volumes of each eluate were processed for immunoblotting to detect the indicated proteins.

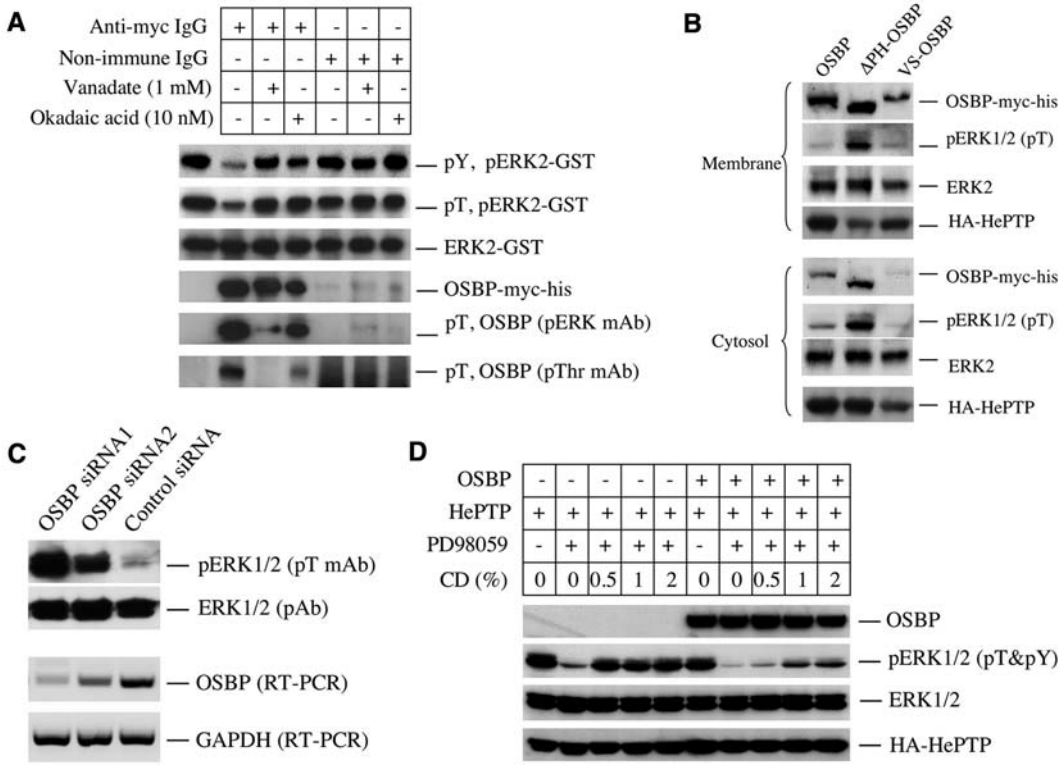

Fig. 4. OSBP oligomer regulates pERK phosphorylation. (**A**) Cytosol was isolated from HeLa cells expressing both OSBP-myc-his and HA-HePTP. Equal amounts of cytosol were processed for immunoprecipitation using either α-myc or nonimmune IgG. The beads were washed and resuspended in buffer C before adding 50 ng of pERK2-GST protein and the indicated inhibitors and incubated for 3 hours at 30°C. The reaction was stopped by adding 6 x SDS sample buffer to the mixture and processing the sample for immunoblotting using antibodies that detect the indicated protein. (**B**) HeLa cells coexpressing HePTP and either wild-type OSBP, ΔPH-OSBP, or VS-OSBP were fractionated into either a membrane fraction or a cytosol fraction and processed for immunoblotting (50 μg per lane) using the indicated antibodies. We used a sensitive pT α-pERK to detect activated ERK. (**C**) HeLa cells were incubated for 24 hours in the presence of two siRNAs directed against different regions of the OSBP mRNA and one directed against the mRNA for microsomal triglyceride transfer protein, and then the cells were washed and cultured for an additional 48 hours before being processed. Cell lysates were then tested for the level of OSBP and glyceraldehyde-phosphate dehydrogenase mRNA with RT-PCR or for the amount of pERK and ERK by immunoblotting. (**D**) HeLa cells expressing either HePTP alone or together with OSBP were cultured in six-well plates for 48 hours. The cells were washed and incubated in serum-free Dulbecco's modified Eagle's medium in the presence of 20 μM PD98059 to block MEK-1 for 10 min at 37°C before adding the indicated amount of CD and incubating an additional 15 min at 37°C. Cells were immediately dissolved in SDS sample buffer and processed for immunoblotting to detect the indicated protein or epitope.

appears to depend on a direct interaction between OSBP and sterols. OSBP belongs to a group of proteins that share in common a phosphoinositide-binding PH domain that can target the molecule to the Golgi apparatus (*8*), a FFAT motif that can target it to the endoplasmic reticulum (ER) (*9*), and a lipid-binding domain that binds specific lipids. These proteins are thought to be involved in the nonvesicular transfer of lipids between various membrane compartments (*10*). For example, CERT has recently been identified as a ceramide-binding protein that appears to use the PH and FFAT motifs to transfer ceramide between ER and Golgi-apparatus membranes (*11*). Although a nonvesicular lipid transport function has not been established for OSBP, it does move to the Golgi apparatus when cells are either depleted of cholesterol or exposed to oxysterols, which indicates that it has the ability to sense cellular sterol levels. Targeting to the Golgi apparatus depends on the PH domain (*12*). OSBP also can bind VAP in ER membranes (*13*). Ordinarily, most of the OSBP appears to be soluble in the cytoplasm in a conformation that masks the PH domain (*8*).

If OSBP is the cholesterol-sensing protein in the pERK phosphatase oligomer, then we imagine that when cholesterol binds to the lipid-binding domain in OSBP it undergoes a conformational change that masks the PH domain. In this configuration, OSBP is able to bind HePTP and PP2A to form a high-molecular-weight complex (fig. S6A). The molecules in the oligomer are precisely arranged so that they are able to interact in response to specific environmental cues. These interactions are critical for spatially organizing HePTP and PP2A so that they can work coordinately to remove both phosphates from pERK1/2 but not from other mitogen-activated protein kinases such as stress-activated protein kinase (*2*). Either oxysterol binding or cholesterol removal changes the conformation of OSBP so that the PH domain is exposed and the phosphatases dissociate (fig. S6B). Unmasking the PH domain causes OSBP to move to specific membrane compartments such as the Golgi apparatus, where it may reacquire cholesterol. Therefore, the pERK1/2 phosphatase activity conferred through OSBP is positively regulated by cholesterol and negatively regulated by oxysterols. One implication of this model is that other lipid-transfer proteins with pH domains and FFAT motifs may have lipid-specific scaffolding functions that regulate key signaling pathways.

References and Notes

1. T. Furuchi, R. G. Anderson, *J. Biol. Chem.* **273**, 21099 (1998).
2. P. Y. Wang, P. Liu, J. Weng, E. Sontag, R. G. Anderson, *EMBO J.* **22**, 2658 (2003).
3. K. A. Augustine *et al.*, *Anat. Rec.* **258**, 221 (2000).
4. R. Pulido, A. Zuniga, A. Ullrich, *EMBO J.* **17**, 7337 (1998).
5. M. K. Storey, D. M. Byers, H. W. Cook, N. D. Ridgway, *Biochem. J.* **336**, 247 (1998).
6. M. P. Ares *et al.*, *Atherosclerosis* **153**, 23 (2000).
7. J. H. Yoon, A. E. Canbay, N. W. Werneburg, S. P. Lee, G. J. Gores, *Hepatology* **39**, 732 (2004).
8. N. D. Ridgway, P. A. Dawson, Y. K. Ho, M. S. Brown, J. L. Goldstein, *J. Cell Biol.* **116**, 307 (1992).
9. C. J. Loewen, A. Roy, T. P. Levine, *EMBO J.* **22**, 2025 (2003).
10. S. Munro, *Nature* **426**, 775 (2003).
11. K. Hanada *et al.*, *Nature* **426**, 803 (2003).
12. A. Mohammadi *et al.*, *J. Lipid Res.* **42**, 1062 (2001).
13. J. P. Wyles, C. R. McMaster, N. D. Ridgway, *J. Biol. Chem.* **277**, 29908 (2002).

14. We thank C. Hall and M. Zhu for valuable technical assistance and B. Pallares for administrative assistance. We are indebted to E. Sontag for advice and reagents. This work was supported by NIH (HL 20948, GM 52016), the Perot Family Foundation, and the Cecil H. Green Distinguished Chair in Cellular and Molecular Biology. Molecular interaction data have been deposited in the Biomolecular Interaction Network Database with accession code 196938.

Supporting Online Material

www.sciencemag.org/cgi/content/full/307/5714/1472/DC1
Materials and Methods
Figs. S1 to S6
Table S1
References

19 November 2004; accepted 7 January 2005
10.1126/science.1107710

How Visual Stimuli Activate Dopaminergic Neurons at Short Latency

Eleanor Dommett,[1]* Véronique Coizet,[1]* Charles D. Blaha,[2]† John Martindale,[1] Véronique Lefebvre,[1] Natalie Walton,[1] John E. W. Mayhew,[1] Paul G. Overton,[1] Peter Redgrave[1]‡

Unexpected, biologically salient stimuli elicit a short-latency, phasic response in midbrain dopaminergic (DA) neurons. Although this signal is important for reinforcement learning, the information it conveys to forebrain target structures remains uncertain. One way to decode the phasic DA signal would be to determine the perceptual properties of sensory inputs to DA neurons. After local disinhibition of the superior colliculus in anesthetized rats, DA neurons became visually responsive, whereas disinhibition of the visual cortex was ineffective. As the primary source of visual afferents, the limited processing capacities of the colliculus may constrain the visual information content of phasic DA responses.

Sensory stimuli that are biologically salient because of their novelty, intensity, or reward value elicit a stereotyped phasic (short-latency <100 ms; short-duration ~100 ms) increase in firing rate of midbrain DA neurons in a variety of mammals (*1–3*). If not reinforced, responses to novel stimuli become habituated rapidly. The responses to rewarding stimuli also decline if stimuli can be predicted. When reward is signaled by an arbitrary stimulus, the phasic DA response shifts from the primary reward to the predicting stimulus. If, under these circumstances, a predicted reward fails to materialize, there is a brief pause in the ongoing activity of DA neurons. These findings have led to the influential suggestion that DA neurons provide the brain's reinforcement learning mechanisms with a "reward prediction error" signal that may be used to adjust future behavioral response probabilities (*4–6*). However, DA neurons exhibit robust responses to a wider class of stimuli than those unambiguously related to reward (*2*, *7*); this suggests that the phasic DA signal may have a broader role than reward alone (*8*). An important strategy for decoding the phasic DA signal would be to identify and then to elucidate the perceptual properties of the sensory pathways providing input to DA neurons. Surprisingly, very little is known about the source(s) of the short-latency phasic sensory input to DA neurons. A candidate structure is the superior colliculus, a retino-recipient nucleus in the dorsal midbrain with direct efferent projections to dopamine-containing regions of the ventral midbrain (*9*). The experimental rationale of the present study was based on a recent report (*10*) that, in the deep layers of the superior colliculus, which project directly to DA neurons (*9*), visual sensitivity is suppressed by anesthesia and can be restored temporarily by local injections of disinhibitory pharmacological agents.

Simultaneous electrophysiological recordings from the superior colliculus deep layers and electrophysiologically identified DA neurons in the substantia nigra (N = 18), or ventral tegmental area (N = 17), of anesthetized rats (*11*) revealed in all cases (N = 35)

[1]Department of Psychology, University of Sheffield, Sheffield, S10 2TP, UK. [2]Department of Psychology, Macquarie University, Sydney, NSW 2109, Australia.

*These authors contributed equally to this work.
†Present address: Department of Psychology, University of Memphis, Memphis, TN 38152–3230, USA.
‡To whom correspondence should be addressed. E-mail: P.Redgrave@sheffield.ac.uk